Aggregation of Surfactant Squaraine Dyes in Aqueous Solution and Microheterogeneous Media: Correlation of Aggregation Behavior with Molecular Structure

Huijuan Chen,[†] Mohammad S. Farahat,[†] Kock-Yee Law,*[,§] and David G. Whitten*[,†]

Contribution from the NSF Center for Photoinduced Charge Transfer, Department of Chemistry, University of Rochester, Rochester, New York 14627, and Xerox Corporation, Wilson Center for Research and Technology, 800 Phillips Road, 114-39D, Webster, New York 14580

Received July 19, 1995[⊗]

Abstract: The synthesis of several amphiphilic squaraine dyes and a study of their aggregation behavior and photophysics are reported. The several different squaraines are found to give spectrally blue-shifted aggregates in aqueous and mixed aqueous-organic solution and in microheterogeneous media (bilayer vesicles). While in some cases an intermediate dimer can be detected in the monomer to aggregate conversion process, in others direct conversion of monomer to aggregate is observed. The aggregation number can be determined together with the equilibrium constant and thermodynamic parameters for some of the squaraines in different environments. In several cases the aggregation number is found to be *ca.* 4. The finding of a strong induced circular dichroism signal when the aggregate (but not dimer or monomer) is generated in the presence of a chiral host (or counterion) suggests that the aggregate is chiral. From these results and molecular simulations indicating that an extended monolayer of some of the squaraines adopts a glide or herringbone lattice we propose a chiral "pinwheel" structure for the unit aggregate and suggest that extended aggregate structures or crystals may be a mosaic of these unit aggregates. In contrast to the monomers, which are strongly fluorescent, the squaraine dimers and aggregates are nonfluorescent and have extremely short exciton lifetimes, as indicated by transient spectroscopy.

Introduction

Squaraine dyes are intriguing compounds both due to their unusual electronic structures as well as to their properties as semiconductors and photogeneration materials in electrophotography.[1] Most applications using squaraine derivatives employ them as solids, usually microcrystalline, in which there is clear indication that the squaraine chromophores are aggregated.[1,2] Several studies have shown that squaraines can exist as different kinds of aggregates, with at least two prominent limiting forms commonly occurring.[3−5] In a recent study, the type of aggregation for a number of squaraines has been shown to depend on the structure of the chromophores in mixed-solvent experiments.[6] Studies of crystalline solids show, for example, that bis(4-methoxyphenyl)squaraine exists in the solid as a "card pack" array in which the planar squaraines are stacked vertically.[7] This structure exhibits a spectrum strongly blue-shifted compared to that of the monomer in dilute solution.[2] In contrast, bis(2-methyl-4-(dimethylamino)phenyl)squaraine forms crystals in which the squaraine chromophores are in a "slipped stack" arrangement; in this case the crystals show a prominent transition strongly red-shifted compared to the solution monomer.[8] The behavior of other solid squaraines usually shows one of these characteristic spectroscopic features—blue-shifted corresponding to an "H" aggregate or red-shifted characteristic of a "J" aggregate, respectively.[9,10] Since the classical exciton treatments of Kasha and Hochstrasser[11,12] and Kuhn and co-workers[13,14] predict shifts similar to those observed in the crystals for molecular arrangements in aggregates, it is reasonable to assume that many squaraine aggregates exhibiting similar absorption spectra in microcrystals,[7−10] films,[3,15,16] or other media[17] may show similar intermolecular arrangements. Interestingly, we have found that several surfactant or amphiphilic squaraines form stable monolayer films at the air−water interface that can be transferred to optically transparent rigid supports.[15,18] Not surprisingly we find that most of the freshly prepared Langmuir−Blodgett (LB) films of these squaraines show blue-shifted or "H" aggregates which would be anticipated if the molecules are arranged in the film in a simple "card-pack" array. However, in a number of cases we have found that heating of these films results in their conversion to a red-shifted aggregate, a process which may be reversed by heating the product films in a humid atmosphere.[3,15] We have also carried out Monte Carlo simulations on some of these squaraine amphiphiles which suggest that the most stable arrangement in a monolayer film is a glide or "herringbone" lattice in which a more complex arrangement than a simple card pack is present.[15,19] Calculations of the exciton shifts for such a structure predict a blue-shift for the

* Authors to whom correspondence should be addressed.
[†] University of Rochester.
[§] Xerox Corporation.
[⊗] Abstract published in *Advance ACS Abstracts,* March 1, 1996.
(1) Law, K. Y. *Chem. Rev.* **1993**, *93*, 449.
(2) Law, K. Y. *J. Phys. Chem.* **1988**, *92*, 4226.
(3) Liang, K.; Law, K. Y.; Whitten, D. G. *J. Phys. Chem.* **1994**, *98*, 13379.
(4) Buncel, E.; McKerrow, A.; Kazmaier, P. M. *J. Chem. Soc., Chem. Commun.* **1992**, 1242.
(5) Das, S.; Thanulingam, T. L.; Thomas, K. G.; Kamat, P. V.; George, M. V. *J. Phys. Chem.* **1993**, *97*, 13620.
(6) McKerrow, A. J.; Buncel, E.; Kazmaier, P. M. *Can. J. Chem.* **1995**, *73*, 1605.
(7) Farnum, D. G.; Neuman, M. A.; Suggs, W. T., Jr. *J. Cryst. Mol. Struct.* **1974**, *4*, 199.
(8) Wingard, R. E. *IEEE Ind. Appl.* **1982**, 1251.
(9) Tristani-Kendra, M.; Eckhardt, C. J. *J. Chem. Phys.* **1984**, *81*, 1160.
(10) Bernstein, J.; Goldstein, E. *Mol. Cryst. Liq. Cryst.* **1988**, *164*, 213.
(11) Kasha, M.; Rawls, H. R.; El-Bayoumi, M. *Pure Appl. Chem.* **1965**, *11*, 371.
(12) Hochestrasser, R. M.; Kasha, M. *Photochem. Photobiol.* **1964**, *3*, 317.

0002-7863/96/1518-2584$12.00/0

allowed transition similar to that actually observed in the freshly prepared LB films.[19]

In recent studies of aggregates of other chromophores, most notably those formed from *trans*-stilbene[20,21] and *trans*-azobenzene,[22] we have found that while extended aggregates occur, there is a relatively small "unit" aggregate structure in several cases that is cyclic, chiral, and relatively stable. These studies to date suggest that even extended arrays of aggregate are probably best described as mosaics of the unit aggregate. For both the *trans*-stilbene aggregate and the corresponding *trans*-azobenzene, the unit structure can be thought of as a piece of a larger glide lattice. Hence it seemed of interest to examine the aggregates formed from amphiphilic squaraines under conditions which might favor formation of a "unit" aggregate.

Since the two types of aggregates generated in the films show quite different photophysical properties which should reflect very different photogeneration efficiencies,[2,23] it would be of interest to correlate how stability and structure of the aggregates correlates with changes in structure of the component squaraine molecule. Accordingly we have synthesized a series of squaraine amphiphiles which should vary chiefly in how they can assemble in films and related microheterogeneous media. In the present paper we report a study of these squaraines in aqueous and mixed aqueous-organic solutions and in microheterogeneous media such as aqueous phospholipid vesicles. In all of these solution media we can observe the transition between monomer and aggregate; together these studies provide a picture of the "unit aggregate structure" for the squaraines, which is likely the precursor for the extended aggregate in crystals or LB films. Since these solution aggregates can be easily studied by conventional solution techniques, these studies also provide a useful picture of the structure and photophysical properties of the squaraine aggregates. Our results indicate that the squaraine unit aggregate may be a similar cyclic chiral structure to those observed with other rod-like chromophores incorporated into amphiphile structures.[21,22]

Experimental Section

Materials and General Techniques. Synthetic reagents were generally purchased from Aldrich Chemical Company and used as received unless specifically stated. α-, β-, and γ-cyclodextrins (99+%), L,D-α-alanine (99%), potassium phosphate (monobasic and dibasic, 99%), dioctadecyldimethylammoniumbromide were purchased from Aldrich. L-α-Dimyristoyl-phosphatidylcholine (DMPC, 99+%) and D, L, and DL-α-dipalmitoylphosphatidylcholine (DPPC, 99%) were purchased from Sigma and tributyl orthoformate from Pfaltz & Bauer. Diethyl ether (anhydrous), *N*,*N*-dimethylformamide, 2-propanol, methanol, ethyl acetate, hexane, methylene chloride, chloroform, dimethyl sulfoxide, and concentrated hydrochloric acid were certified grade from Fisher. All solvents for spectroscopic studies were spectroscopic grade from Fisher or Aldrich. Suitable water was obtained by passing purified in-house distilled water through a Millipore-RO/UF water purification system. Deuterated solvents were purchased from MSD Isotopes or Cambridge Isotope Laboratories.

Melting points were taken on a Mel-Temp II melting point apparatus and were uncorrected. Potassium phosphate solutions (10 mM, both monobasic and dibasic) were used to adjust the pH to 7.5 in aqueous solution studies in the cases when it was necessary. The pH values were measured with an Orion Research digital ionalyzer/501 pH meter. Infrared spectra were obtained on a Matheson Galaxy 6020 FTIR. Proton NMR spectra were recorded on a General Electric QE300 MHz spectrometer using deuterated solvent locks. FAB mass spectra were measured at the Midwest Center of Mass Spectrometry. Elemental analyses were performed by Galbraith Laboratories, Inc. (Knoxville, TN) or Desert Analytics (Tucson, AZ). Absorption spectra for both solution and solid state studies were obtained on a Hewlett-Packard 8452A diode array spectrophotometer. The circular dichroism study was carried out on a JASCO J-710 spectropolarimeter. Fluorescence spectra were recorded on a SPEX Fluorolog-2 spectrofluorometer and are uncorrected.

Bilayer vesicles were prepared according to reported procedures.[24] Solutions of squaraine or mixtures of squaraine and phospholipid in chloroform were transferred to a scintillation vial; the solvent was evaporated by flushing with nitrogen, the residue in the vial was dried in a vacuum desiccator overnight. An appropriate volume of Mili-Q water was added to the vial, and the temperature was controlled at ∼70 °C for 10 min in order to hydrate the residue. The mixture was then sonicated with a Cell Disrupter W220F from Heat Systems-Ultrasonics, Inc. (setting 6.5, 35 w) for three 5 min periods with an intervening 5 min delay for cooling. The stock vesicle solution was centrifuged for 30 min at 3500 rpm using a Fisher Scientific centrifuge; the top portion of solution was carefully taken out with a pipette. Size extrusion experiments for vesicle systems were performed with an extruder through CoStar Nuclepore Polycarbonate (PC) filters. Light scattering measurements were carried out at 20 °C, and all samples were routinely filtered through a 1.2 μm nylon syringe filter before data acquisition.[25]

Fluorescence Lifetime Measurements. Time-correlated single photon counting (TCSPC) experiments were carried out on an instrument consisting of a mode-locked Nd:YLF laser (Quantronix 4000 Series) operating at 76 MHz as the primary laser source. The second harmonic (KTP crystal) of the Nd:YLF laser was used to synchronously pump a dye laser (Coherent 700) circulating Rhodamine 6G in ethylene glycol as the gain medium. The pulsewidth of the dye laser was typically 8 ps, as determined by auto-correlation, and was cavity dumped at a rate of 1.9 MHz. The dye laser was tuned to the desired wavelength for sample excitation (575−605 nm). Photon flux of laser pulses were typically less than 10^{11} photons/cm^2. Emission from the sample was collected by two convex lenses and focused at the entrance slit of a Spex 1681 monochromator (0.22 m) and was detected by a red-sensitive multichannel plate (MCP) detector (Hamamatsu R3809U−01). The single photon pulses from the MCP detector were amplified and used as the start signal for a time-to-amplitude converter (TAC, EG&G Ortec), while the signal from a photodiode, detecting a small fraction of the dye laser output, was used as the stop signal for the TAC. The start and stop signals for the TAC were conditioned before entering the TAC by passing through two separate channels of a constant fraction discriminator (CFD, Tennelec TC 454). The output of the TAC was connected to a multichannel analyzer (MCA) interface board (Norland 5000) installed inside a 486DX2 personal computer. The MCA was controlled by software from Edinburgh Instruments (Edinburgh, UK). The same software was used to carry out the deconvolution of the data and exponential fitting using the nonlinear least squares method. Measurements were made on air saturated samples at the magic angle (55°).

Transient Absorption Measurements. A mode-locked Nd:YAG laser (Continuum PY61C) with 25−35 ps 1064 nm fundamental pulses (10 Hz) was used as the pump and the probe sources for transient absorption measurements. The fundamental was passed through a

(13) V. Czikkely, H.; Försterling, H. D.; Kuhn, H. *Chem. Phys. Lett.* **1970**, *6*, 11.
(14) V. Czikkely, H.; Försterling, H. D.; Kuhn, H. *Chem. Phys. Lett.* **1970**, *6*, 207.
(15) Chen, H., Herkstroeter, W. G.; Perlstein, J.; Law, K. Y.; Whitten, D. G. *J. Phys. Chem.* **1994**, *98*, 5138.
(16) Law, K. Y.; Chen, C. C. *J. Phys. Chem.* **1989**, *93*, 2533.
(17) Das, S.; Thomas, K. G.; George, M. V.; Kamat, P. V. *J. Chem. Soc., Faraday Trans.* **1992**, *88*, 3419.
(18) Chen, H.; Law, K. Y.; Perlstein, J.; Whitten, D. G. Manuscript in preparation.
(19) Chen, H.; Law, K. Y.; Perlstein, J.; Whitten, D. G. *J. Am. Chem. Soc.* **1995**, *117*, 7257.
(20) Song, X, Geiger, C.; Furman, I.; Whitten, D. G. *J. Am. Chem. Soc.* **1994**, *116*, 4103.
(21) Song, X.; Geiger, C.; Leinhos, U.; Perlstein, J.; Whitten, D. G. *J. Am. Chem. Soc.* **1994**, *116*, 10340.
(22) Song, X.; Perlstein, J.; Whitten, D. G. *J. Am. Chem. Soc.* In press.
(23) Kim, Y. S.; Liang, K.; Law, K. Y.; Whitten, D. G. *J. Phys. Chem.* **1994**, *98*, 984.
(24) Hope, M. J.; Bally, M. B.; Webb, G.; Cullis, P. R. *Biophys. Acta* **1985**, *55*, 812.
(25) The authors thank Dr. Thomas Whitesides for the light scattering measurements.

computer controlled variable optical delay line (Velmex) to achieve the desired delay between pump and probe beams. The second harmonic wavelength of the laser (532 nm) was used as the excitation source for most experiments. For experiments requiring longer excitation wavelengths, Raman shifting of the 532 nm beam in acetone−d_6 was used to obtain 600 nm excitation pulses. The excitation beam diameter was ∼2 mm. After the delay line the fundamental pulse was focused into a 10 cm cell with quartz windows containing H_2O/D_2O (1:1) for white light continuum generation. The white light was collimated after the cell and focused at one end of a 200 μm fused silica optical fiber. The white light was recollimated after exiting the second end of the optical fiber and was split 50/50 by a cube beamsplitter after passing through a polarization descrambler. One beam was used as the reference, and the other was used as the interrogation beam passing through the sample cell after reducing the beam diameter to ∼1.5 mm by a lens. The two beams were recollimated and focused at the ends of a bifurcated fiber optic pair that was attached to a SPEX 270 monochromator. The spectra of the white light continuum for the sample and reference beams with and without excitation were detected after passing through the monochromator by a cooled dual diode array detector (Princeton Instruments ST121/DDA512), and corresponding differential absorption spectra at the set delay time were calculated, displayed, and stored on disk by a BASIC program.

For kinetics measurements, the second output of the monochromator was used and the monitoring beams were detected by two miniphotomultiplier tubes (Hamamatsu HC120) and digitized by a LeCroy digital oscilloscope before being available to a BASIC program for data manipulation and storage. Sample solutions in 1 cm pathlength cells were used with typical pulse energies of 100−500 μJ, except when nonlinear laser intensity dependence was observed. In latter cases pulse energies of <50 μJ (<2 × 10^{15} photo/cm^2 at 532 nm) were used. The instrument response was 35−40 ps (FWHM) depending on the mode−locking dye used. The spectra showed evolution in time of ∼4 nm/ps (positive chirp) due to the use of the fiber optic piece for delivery of the white light continuum to the sample. The positive chirp caused the shorter wavelengths of the spectra to appear before the longer wavelengths; however, it did not affect the single wavelength kinetics measurements. Prolonged and repetitive experiments for vesicle solutions at the highest laser intensities used led to a decrease in the ground state absorption (permanent bleaching) for **8814DHA** and **88DHT**. Reported data are for fresh vesicle solutions of these dyes with minimum permanent bleaching (<2%).

Synthesis of Squaraines. 4-(*N*-methyl-*N*-(carboxypropyl)amino)-phenyl-4′-(*N*,*N*-dimethylamino)phenylsquaraine (1114A). *N*-methyl-*N*-(carboxypropyl)aniline (prepared according to a previous procedure,[15] 0.53 g, 2.76 mmol), 2-propanol (25 mL), and tributyl orthoformate (2 mL) were placed in a three-necked, 100 mL flask with a magnetic stirbar. The mixture was stirred and brought to reflux under nitrogen atmosphere. A solution containing 1-(*p*-dimethylaminophenyl)-2-hydroxycyclobutene-3,4-dione (previously prepared,[26] 0.30 g, 1.38 mmol) in ∼2 mL of DMSO was added evenly through a pressure equalizing funnel over a 3-h period. The mixture was kept at reflux for an additional 2 h after the addition was completed. A blue precipitate was isolated by filtration. After washing the precipitate with cold 2-propanol and ether, the blue solid was vacuum dried. Pure squaraine **1114A** was separated from the crude product by dissolving in hot chloroform with a Soxhlet extractor: 0.15 g (yield 28%) blue solid was obtained after drying in vacuum oven (70 °C), mp 245−246 °C; ^{1}H NMR (DMSO-d_6) δ 8.14−8.12 (dd, 4H), 6.82−6.70 (dd, 4H), 3.57 (t, 2H), 3.20 (s, 6H), 3.12 (s, 3H), 2.32 (t, 2H), 1.81 (m, 2H); IR (KBr) 1589 cm^{-1}, 1734 cm^{-1}; UV−visible λ_{max} ($CHCl_3$) 628 nm, ϵ_{max} = 2.95 × 10^5 M^{-1} cm^{-1}; FAB mass obsd *m/z* 393.1983 (M + H), mass calcd for $C_{23}H_{24}O_4N_2$ 392.1836.

4-(*N*-methyl-*N*-(carboxypropyl)amino)phenyl-4′-(*N*,*N*-dibutylamino)phenylsquaraine (4414A) was reported in a previous study.[15]

***N*,*N*-Dioctylaniline.** *N*,*N*-Dioctylaniline was prepared according to the procedure used by Desai.[27] Aniline (2.5 g, 27 mmol), bromooctane (18.2 g, 94 mmol), and 80 mL of butanol were heated at ∼100 °C in the presence of 4.4 g of sodium carbonate and 0.12 g of iodine for 24 h. The reaction mixture was then cooled to room temperature. The crude product was dissolved in water and then was extracted with ether. The combined extract was washed with water, dried over $MgSO_4$, evaporated to remove solvent, and isolated by vacuum distillation. Pure *N*,*N*-dioctylaniline was isolated as a clear liquid: yield 5.48 g (65%); bp 170−172 °C at 2 mmHg; ^{1}H NMR ($CDCl_3$) δ 7.25 (t, 2H), 6.75 (m, 3H), 3.32 (t, 4H), 1.62 (m, 4H), 1.35(m, 20H) and 0.92 (t, 6H).

1-Chloro-2-(*p*-dioctylaminophenyl)cyclobutene-3,4-dione. 1-Chloro-2-(*p*-dioctylaminophenyl)cyclobutene-3,4-dione was synthesized according to the procedure used by Wendling *et al*.[28] A solution of 1,2-dichlorocyclobutene-3,4-dione (1.19 g, 7.9 mmol, freshly prepared according to a reported procedure[29]) and *N*,*N*-dioctylaniline (2.5 g, 7.9 mmol) in 8 mL of methylene chloride was added dropwise to a methylene chloride solution of the catalyst (1.05 g, 7.9 mmol of $AlCl_3$ in 30 mL CH_2Cl_2) at reflux. The mixture was refluxed for an hour after addition. The product solution was poured into 50 mL of ice water containing 2 drops of concentrated HCl. The organic layer was separated, washed with water, dried over $MgSO_4$, filtered, and evaporated. The pure product (1.05 g) was obtained as light yellow crystals by flash column chromatography on silica gel (70−230 mesh), with ethyl acetate/hexane = 1:20 as eluent: yield: 30.5%; mp 79−80 °C; IR (KBr) 1795, 1608, 1572 cm^{-1}; ^{1}H NMR ($CDCl_3$) δ 8.15 (d, 2H), 6.73 (d, 2H), 3.41 (t, 4H), 1.64 (m, 4H), 1.30 (m, 20H) and 0.90 (t, 6H); UV−visible λ_{max} ($CHCl_3$) 416 nm.

1-(*p*-Dioctylaminophenyl)-2-hydroxycyclobutene-3,4-dione. 1-Chloro-2-(*p*-dioctylaminophenyl)cyclobutene-3,4-dione (1.0 g, 2.31 mmol) was suspended in 50 mL of 18% HCl solution. The mixture was brought to reflux for 2 h and was cooled to room temperature. The top organic layer, a yellow liquid, was decanted into a round-bottomed flask. After evaporation of the solvent, a brown residue was obtained. The brown solid was washed with water (3 × 20 mL) and was recrystallized from a mixture of DMSO (∼3 mL) and water (20 mL). A light yellow solid was isolated by filtration, washed with ether (3 × 5 mL), and vacuum dried at 60 °C overnight: yield 0.93 g (98%); mp 199−200 °C; IR (KBr) 1768 cm^{-1}, 1577 cm^{-1}; ^{1}H NMR (DMSO-d_6) δ 7.84 (d, 2H), 6.61 (d, 2H), 3.26 (t, 4H), 1.48 (m, 4H), 1.24 (m, 20H) and 0.83 (t, 6H); FAB mass obsd *m/z* 414.3012 (M + H), mass calcd for $C_{26}H_{40}O_3N$ 414.3008.

4-(*N*-Methyl-*N*-(carboxypropyl)amino)phenyl-4′-(*N*,*N*-dioctylamino)phenylsquaraine (8814A). *N*-Methyl-*N*-(carboxypropyl)aniline (0.47 g, 2.42 mmol) was reacted with 1-(*p*-dioctylaminophenyl)-2-hydroxycyclobutene-3,4-dione (0.50 g, 1.21 mmol) in the presence of tributyl orthoformate (1.8 mL) in 2-propanol (25 mL) for ∼3 h. A blue precipitate was isolated by filtration. After having been washed with 2-propanol and ether, the blue solid was vacuum dried and purified by recrystallization from MeOH/CH_2Cl_2: yield 0.25 (35%); mp 202−203 °C dec; ^{1}H NMR ($CDCl_3$) δ 8.38−8.35 (dd, 4H), 6.82−6.70 (dd, 4H), 3.59 (t, 2H), 3.43 (t, 4H), 3.16 (s, 3H), 2.50 (t, 2H), 2.04 (m, 2H), 1.66 (m, 4H), 1.35−1.40 (m, 20H) and 0.90 (t, 6H); IR (KBr) 1588 cm^{-1}, 1735 cm^{-1}; UV−visible λ_{max} ($CHCl_3$) 634 nm, ϵ_{max} = 3.12 × 10^5 M^{-1}cm^{-1}. Anal. Calcd ($C_{37}H_{52}O_4N_2$): C, 75.47; H, 8.90; N, 4.76; O, 10.87. Found: C, 75.51; H 8.81; N, 4.57.

***N*,*N*-Bis(carboxypropyl)aniline.** Aniline (5.0 g, 54 mmol) and ethyl 4-bromobutyrate (19.0 g, 120 mmol) in 50 mL of butanol were heated at ∼100 °C for 16 h in the presence of 8.0 g of sodium carbonate and 0.10 g of iodine. The reaction mixture was then cooled to room temperature, dissolved in water, and extracted with ether. The combined extract was washed with water, dried over $MgSO_4$, evaporated to remove solvent, and isolated by vacuum distillation. Pure *N*,*N*-di-(ethyl 4-butanoate)aniline was isolated as an oily liquid: Yield 8.7 g (50%); bp 167−170 °C at 2 mmHg; ^{1}H NMR ($CDCl_3$) δ 7.25 (t, 2H), 6.75 (m, 3H), 4.168(q, 4H), 3.37 (t, 4H), 2.38 (t, 4H), 1.95 (m, 4H) and 1.26 (t, 6H).

The ester product (8 g, 24.9 mmol) was then hydrolyzed in 150 mL of 5% KOH and refluxed for 2 h. After cooling to room temperature, the reaction mixture was washed with ether (2 × 60 mL), the aqueous layer was then adjusted to pH 5.5 with concentrated hydrochloric acid,

(26) Law, K. Y.; Bailey, F. C. *Can. J. Chem.* **1993**, *71*, 494.
(27) Desai, R. D. *J. Indian Inst. Sci.* **1924**, *7*, 235.
(28) Wendling, L. A.; Koster, S. K.; Murry, J. E.; West, R. *J. Org. Chem.* **1977**, *42*, 1129.
(29) De Selms, C. D.; Fox, C. J.; Riordan, R. C. *Tetrahedron Lett.* **1970**, 781.
(30) Kunitake, T. *Angew. Chem., Int. Ed. Engl.* **1992**, *31*, 709.

extracted with ether (3 × 60 mL), dried over $MgSO_4$, and evaporated to remove solvent. *N*,*N*-Bis(carboxypropyl)aniline was obtained as a solid with a yield of 6.1 g (96%): mp 80−82 °C; ^{1}H NMR ($CDCl_3$) δ 7.26 (t, 2H), 6.76 (m, 3H), 3.40 (t, 4H), 2.45 (t, 4H) and 1.96 (m, 4H).

4-(*N*,*N*-Bis(carboxypropyl)amino)phenyl-4′-(*N*,*N*-dioctylamino)-phenylsquaraine (8844A$_2$). *N*,*N*-Bis(carboxypropyl)aniline (0.64 g, 2.42 mmol) was reacted with 1-(*p*-dioctylaminophenyl)-2-hydroxycyclobutene-3,4-dione (0.50 g, 1.21 mmol) in 2-propanol (20 mL) in the presence of tributyl orthoformate (1.8 g) for ∼4 h. A blue precipitate was isolated by filtration. After washing with 2-propanol and ether, the blue solid was vacuum dried and was purified by recrystallization from DMSO/CH_2Cl_2: yield 0.21 (26.3%); mp 183−184 °C dec; ^{1}H NMR ($CDCl_3$) δ 8.40−8.36 (dd, 4H), 6.90−6.75 (dd, 4H), 3.55 (t, 4H), 3.43 (t, 4H), 2.50 (t, 4H), 1.96 (m, 4H), 1.68 (m, 4H), 1.35−1.40 (m, 20H) and 0.90 (t, 6H); IR (KBr) 1587 cm^{-1}, 1735 cm^{-1}; UV−visible λ_{max} ($CHCl_3$) 638 nm, $\epsilon_{max} = 2.21 \times 10^5$ M^{-1} cm^{-1}. Anal. Calcd ($C_{40}H_{56}O_6N_2$): C, 72.70; H, 8.54; N, 4.24; O, 14.53. Found: C, 72.34; H, 8.58; N, 3.99.

***N*-(Ethyl 4-butanoate)-3,5-dimethoxyaniline.** 3,5-Dimethoxyaniline (10.1 g, 65.9 mmol), ethyl 4-brombutyrate (4.95 g, 25.4 mmol), and 80 mL of butanol were heated at ∼70 °C in the presence of 3.0 g of sodium acetate for 10 h. The reaction mixture was then cooled to room temperature. The crude product was dissolved in water and then was extracted with ether. The combined extract was washed with water, dried over $MgSO_4$, evaporated to remove solvent, and isolated by column chromatography on silica gel (70−230 mesh), with ethyl acetate/hexane = 1/2 as eluent. Pure *N*-(ethyl 4-butanoate)aniline was isolated as a white solid: yield 4.82 g (73.6.%); mp 42−43 °C; ^{1}H NMR ($CDCl_3$) δ 5.96 (s, 1H), 5.92 (s, 2H), 4.14 (m, 2H), 3.78 (s, 6H), 3.18 (t, 2H), 2.43 (t, 2H), 1.96 (m, 2H), 1.27 (t, 3H).

***N*-Methyl-*N*-(ethyl 4-butanoate)-3,5-dimethoxyaniline.** *N*-(ethyl 4-butanoate)-3,5-dimethoxyaniline (4.8 g, 18.0 mmol), methyl iodide (2.55 g, 18.0 mmol), and 30 mL of tetrahydrofuran were heated at ∼50 °C in the presence of 1.48 g of sodium acetate for 10 h. The reaction mixture was then cooled, poured into 50 mL of water, and then extracted with ether. The combined extract was washed with water, dried over $MgSO_4$, evaporated to remove solvent, and isolated by column chromatography on silica gel (70−230 mesh), with ethyl acetate/hexane = 1/8 as eluent. Pure *N*-methyl-*N*-(ethyl 4-butanoate)-aniline was isolated as an oily liquid: yield 3.26 g (62.0%); bp 152−153 °C/0.05 mmHg; ^{1}H NMR ($CDCl_3$) δ 5.92 (s, 3H), 4.15 (q, 2H), 3.80 (s, 6H), 3.35 (t, 2H), 2.93 (s, 3H), 2.35 (t, 2H), 1.92 (m, 2H), 1.27 (t, 3H).

***N*-Methyl-*N*-(carboxypropyl)-3,5-dihydroxyaniline.** *N*-Methyl-*N*-(ethyl 4-butanoate)aniline (3 g, 10.7 mmol) was hydrolyzed by refluxing in 50 mL of a 1:1 mixture of acetic acid and hydrobromic acid (47−49%) for 2 h. After cooling to room temperature, the reaction mixture was washed with ethyl acetate (2 × 70 mL), the aqueous layer was then adjusted to pH 5.5 with concentrated sodium hydroxide, extracted with ethyl acetate (3 × 70 mL), dried over $MgSO_4$, and evaporated to remove solvent. *N*-Methyl-*N*-(carboxypropyl)-3,5-dihydroxyaniline was obtained as an oily liquid with a yield of 2.06 g (86%): ^{1}H NMR (DMSO) δ 8.78 (s, 2H), 5.55 (d, 3H), 3.17 (t, 2H), 2.75 (s, 3H), 2.20 (t, 2H) and 1.65 (m, 2H).

4-(*N*-methyl-*N*-(carboxypropyl)amino)phenyl-4′-(*N*,*N*-dibutylamino)-2′,6′-dihydroxyphenylsquaraine (4414DHA). *N*-Methyl-*N*-(carboxypropyl)-3,5-dihydroxyaniline (0.22 g, 0.98 mmol) was reacted with 1-(*p*-dibutylaminophenyl)-2-hydroxycyclobutene-3,4-dione (0.25 g, 0.83 mmol) in glacial acetic acid (25 mL) for ∼3 h. A blue precipitate was isolated by filtration. After having been washed with ether, the blue solid was vacuum dried and purified by recrystallization from acetic acid: yield 0.23 (54.8%); mp 278−280 °C dec; ^{1}H NMR (DMSO-d_6) δ 12.48 (s, 1H), 7.88−7.86 (d, 2H), 6.89−6.86 (d, 2H), 5.91 (s, 2H), 3.59−3.40 (m, 6H), 3.13 (s, 3H), 2.31−2.26 (t, 2H), 1.77−1.72 (m, 2H), 1.58−1.49 (m, 4H), 1.36−1.29 (m, 4H) and 0.90 (t, 6H); IR (KBr) 3458, 1597, 1192 cm^{-1}; UV−visible λ_{max} ($CHCl_3$) 634 nm, $\epsilon_{max} = 2.42 \times 10^5$ M^{-1} cm^{-1}; FAB mass obsd *m*/*z* 508.2570; mass calcd for $C_{29}H_{36}O_6N_2$ 508.2573. Anal. Calcd C, 68.47; H, 7.14; N, 5.51. Found: C, 68.14; H, 7.09; N, 5.71.

4-(*N*-Methyl-*N*-(carboxypropyl)amino)phenyl-4′-(*N*,*N*-dioctylamino)-2′,6′-dihydroxyphenylsquaraine (8814DHA). Similar to the synthesis of **4414DHA**. *N*-Methyl-*N*-(carboxypropyl)-3,5-dihydroxyaniline (0.18 g, 0.80 mmol) was reacted with 1-(*p*-dibutylaminophenyl)-2-hydroxycyclobutene-3,4-dione (0.20 g, 0.48 mmol) in glacial acetic acid (25 mL) for ∼3 h: yield 0.24 (80%); mp 238−240 °C dec; ^{1}H NMR (DMSO-d_6) δ 12.48 (s, 1H), 7.85−7.82 (d, 2H), 6.88−6.85 (d, 2H), 5.91 (s, 2H), 3.49−3.47 (m, 6H), 3.12 (s, 3H), 2.30−2.26 (t, 2H), 1.77−1.73 (m, 2H), 1.54 (m, 4H), 1.27−1.24 (m, 20H) and 0.85 (t, 6H); IR (KBr) 3435 cm^{-1}, 1600 cm^{-1}, 1197 cm^{-1}; UV−visible λ_{max} ($CHCl_3$) 634 nm, $\epsilon_{max} = 2.25 \times 10^5$ M^{-1} cm^{-1}; FAB mass obsd *m*/*z* 620.3825; mass calcd for $C_{37}H_{52}O_6N_2$ 620.3824. Anal. Calcd C, 71.57; H, 8.45; N, 4.51. Found: C, 71.12; H 8.46, N, 4.28.

***N*-Methyl-3,5-dimethoxyaniline.** 3,5-Dimethoxyaniline (6.9 g, 45 mmol), methyl iodide (6.4 g, 45 mmol), and 50 mL of THF were stirred at room temperature in the presence of 3.4 g of sodium acetate for 10 h. The crude product was dissolved in water and then was extracted with ether. The combined extract was washed with water, dried over $MgSO_4$, evaporated to remove solvent, and isolated by column chromatography on silica gel (230−270 mesh), with ethyl acetate/hexane = 1:4 (v/v) as eluent. Pure *N*-methyl-3,5-dimethoxyaniline was isolated as a white solid: yield 2.63 g (35%); ^{1}H NMR ($CDCl_3$) δ 5.90 (s, 1H), 5.82 (s, 2H), 3.76 (s, 6H), 2.83 (s, 3H), 1.96 (m, 2H).

***N*-Methyl-*N*-(8-bromooctyl)-3,5-dimethoxyaniline.** *N*-methyl-3,5-dimethoxyaniline (0.87 g, 5.2 mmol), 1,8-dibromooctane (4.2 g, 15.6 mmol), and 50 mL of butanol were heated at ∼90 °C in the presence of 0.52 g of sodium bicarbonate for 16 h. The crude product was dissolved in water and then was extracted with ether. The combined extract was washed with water, dried over $MgSO_4$, and evaporated to remove solvent, and the product was isolated by column chromatography on silica gel (230−270 mesh), with ethyl acetate/hexane = 1/20 as eluent. *N*-methyl-*N*-(8-bromooctyl)-3,5-dimethoxyaniline (1.86 g) was isolated as a solid: yield (54.8%); ^{1}H NMR ($CDCl_3$) δ 5.89 (s, 3H), 3.80 (s, 6H), 3.42 (t, 2H), 3.28 (t, 2H), 2.92 (s, 3H), 1.86 (m, 2H), 1.34−1.60 (m, 10H).

8-{*N*-(3,5-Dihydroxyphenyl)-*N*-methylamino}octyltrimethyl ammonium Bromide. *N*-methyl-*N*-(8-bromooctyl)-3,5-dimethoxyaniline (1.5 g), was hydrolyzed by refluxing in 50 mL of a 1:1 mixture of acetic acid and hydrobromic acid (47−49%) for 2 h. After having been cooled, the reaction mixture was washed with ethyl acetate (2 × 50 mL), and the aqueous layer was adjusted to pH 6 with concentrated sodium hydroxide, extracted with ethyl acetate (3 × 50 mL), dried over $MgSO_4$, and evaporated to remove the solvent. An oily liquid (*N*-methyl-*N*-(8-bromooctyl)-3,5-dihydroxyaniline) was obtained (yield: 0.83 g, 60%). The oily liquid was dissolved in 10 mL of THF and kept at 0 °C. Trimethylamine was then added to the above solution. The reaction mixture was sealed and stirred at room temperature for 5 h. A white precipitate was formed and isolated by filtration, washed with THF, and dried in vacuum (40 °C): yield: 0.78 g (80%); mp 196 °C; ^{1}H NMR (MeOD) δ 5.72 (s, 2H), 5.66 (s, 1H), 3.34 (t, 2H), 3.20 (t, 2H), 3.11 (s, 9H), 2.84 (s, 3H), 1.76 (m, 4H), 1.50−1.60 (m, 4H), 1.40 (m, 4H).

Squaraine Quaternary Ammonium Bromide 88DHT. Similar to the synthesis of **4414DHA**, 1-(*p*-*N*,*N*-dioctylaminophenyl)-2-hydroxy-3,4-dione (0.15 g, 0.50 mmol) was reacted with 8-{*N*-(3,5-dihydroxyphenyl)-*N*-methylamino}octyltrimethylammonium bromide (0.23 g, 0.60 mmol) in boiling glacial acetic acid for 2 h. A blue precipitate formed after the reaction mixture was cooled down to room temperature. The blue solid was obtained by filtration and was washed with ether, dried in vacuum (50 °C), and further purified by recrystalization from methanol and hexane: yield 0.18 g (64%); mp 166−168 °C dec; ^{1}H NMR ($CDCl_3$) δ 8.07−8.04 (d, 2H), 6.68−6.71(d, 2H), 5.79 (s, 2H), 3.68 (m, 4H), 3.45 (s, 9H), 3.40−3.45 (m, 4H), 3.17 (s, 3H), 1.80−1.30 (m, 36H), 0.92 (t, 3H). IR (KBr) 3459, 1642, 1599, 1183 cm^{-1}; UV−visible λ_{max} ($CHCl_3$) 634 nm, $\epsilon_{max} = 1.78 \times 10^5$ M^{-1} cm^{-1}; HRFAB mass obsd 704.5347 (M^+); mass calcd for $C_{44}H_{70}N_3O_4^+$ 704.5366.

Squaraine Quaternary Ammonium Bromide 48DHT. Similar to the synthesis of **88DHT**. 1-(*p*-*N*,*N*-dibutylaminophenyl)-2-hydroxy-3,4-dione (0.15 g,0.50 mmol) was reacted with 8-{*N*-(3,5-dihydroxyphenyl)-*N*-methylamino}octyltrimethylammonium bromide (0.23 g, 0.60 mmol) in boiling glacial acetic acid for 2 h: yield of the squaraine formation step 63%; mp 178−179 °C dec; ^{1}H NMR ($CDCl_3$) d 8.07−8.04 (d, 2H), 6.68−6.71(d, 2H), 5.79 (s, 2H), 3.68 (m, 4H), 3.45 (s, 9H), 3.40−3.45 (m, 4H), 3.17 (s, 3H), 1.80−1.30 (m, 36H), 0.92 (t,

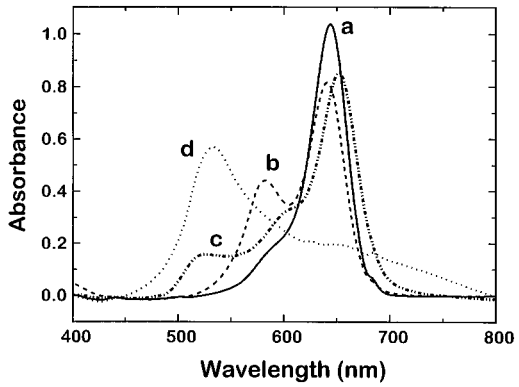

Figure 1. Absorption spectra for type I squaraines in H_2O (pH = 7.5, [dye] = 5×10^{-6} M): (a) **1114A**; (b) **4414A**; (c) **8844A$_2$**; and (d) **8814A**.

3H). IR (KBr) 3457 cm^{-1}, 1640 cm^{-1}, 1598 cm^{-1}, 1182 cm^{-1}; UV−visible λ_{max} ($CHCl_3$) 634 nm, $\epsilon_{max} = 1.81 \times 10^5$ M^{-1} cm^{-1}; FAB mass obsd (M^+) 592.4120; mass calcd for $C_{36}H_{54}N_3O_4^+$ 592.4114.

Results

The series of squaraine amphiphiles is shown in Chart 1. All of these compounds contain hydrophilic head groups, either a carboxylic acid (type I and II) or a quaternary ammonium salt (type III) and various alkyl substituents to render them more or less hydrophobic. Two types of squaraine chromophore are present: in the "type I" squaraines the chromophore is a simple diphenyl squaraine, while for the "type II" and "type III" one of the phenyl rings is dihydroxylated to facilitate intramolecular H-bonding to the squaraine oxygens. In addition, the "type III" squaraines which contain a quaternary ammonium salt as the hydrophilic head group are expected to be capable of forming "pure" squaraine vesicles.[30] All of the compounds with the exception of **1114A** form good LB films which can be transferred to optically transparent supports; in each case the films at the air−water interface and the freshly transferred films show a strong absorption at 520−530 nm, blue-shifted compared to monomer (650 nm in water). The type I squaraines, **4414A** and **8814A**, give conversion to a red-shifted aggregate when their LB films are heated. **8844A$_2$** gives a mixture of red and blue-shifted forms on heating, while the type II squaraines **4414DHA** and **8814DHA** and type III squaraines **48DHT** and **88DHT** also show partial conversion to the red-shifted aggregate. As described in the introduction, the main focus of the present work is the behavior of this series of squaraines in solution and microheterogeneous media.

In Homogeneous Solution. Type I Squaraines. The type I squaraines show only limited solubility in water; however, concentrations on the order of 10^{-5}−10^{-6} M can be obtained in water (pH = 7.5) for short duration (ca 1 h) by injection of a concentrated organic solution of the squaraine into the aqueous or partially aqueous medium in an "arrested crystallization" process. We previously reported that **4414A** forms a mixture of monomer and dimer in water.[15] The structural assignment of the blue-shifted species absorbing at 594 nm was supported by the finding that a similar absorbing species was obtained when aqueous solutions of **4414A** were treated with γ-cyclodextrin. In contrast α- and β-cyclodextrins incorporate only the monomer of **4414A**. For **4414A** a study of the monomer−dimer equilibrium in pure water led to a determination of the thermodynamic parameters for dimer formation of $\Delta H_0^\circ = -6.84$ kcal/mol and $\Delta S_0^\circ = -1.83$ cal/mol deg.[15] As shown in Figure 1, the series of four type I squaraines shows a remarkable contrast in the range of species present in pure water at pH = 7.4 ([squaraine] = 5×10^{-6} M). For **1114A** virtually only the monomer is observed; a small amount of absorption at *ca*. 580 nm is ascribed to the dimer. This is reinforced by the finding that addition of γ-cyclodextrin results in conversion of most of the monomer to this species. In contrast, the squaraines with larger hydrophobic alkyl group substituents exhibit prominent transitions which can be assigned to the dimer (ca. 594 nm) and the aggregate (530 nm). **8814A** exists predominantly as the aggregate with the same maximum (530 nm) as in the LB film while **8844A$_2$** shows both the dimer and the aggregate maxima.

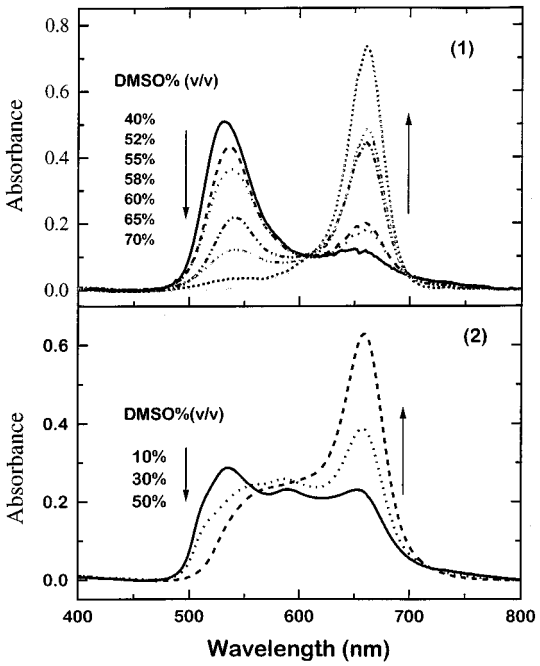

Figure 2. Absorption spectra for squaraines in DMSO−H_2O mixed solvent ([dye] = 5×10^{-6} M): (1) **8814A** and (2) **8844A$_2$**.

Addition of dimethyl sulfoxide (DMSO) to aqueous solutions of the type I squaraines increases their solubility in general and results in a preference for monomer, compared to pure aqueous media. For **1114A** only monomer is observed even at very low (<2%) DMSO content. For the other type I squaraines the interconversion between aggregate, dimer and monomer is observed with increase in DMSO%(v/v); the behavior of these is summarized in Table 1. Figure 2 compares the behavior of **8844A$_2$** and **8814A** over a range of DMSO concentrations. For the former a mixture of aggregate, dimer and monomer is evident over a wide range, while for the latter a clear isosbestic point is observed between aggregate and monomer and no clear maximum corresponding to the dimer is detectable.

Type II and III Squaraines. The addition of two hydroxyl groups to one of the squaraine phenyl rings, such that intramolecular hydrogen bonding with the squaraine oxygens can occur, is anticipated to increase the ease of forming a card-pack aggregate and alter the solubility of the various species encountered above for the type I squaraines. In addition we have found that the type II squaraines have much better long-term stability in the presence of water compared to the type I squaraines and other squaraine dyes, which generally decompose upon prolonged exposure to aqueous media. This can probably be attributed to greater resistance to nucleophilic attack by water on the type II squaraines.[31] The solubility of type II squaraines **4414DHA** and **8814DHA** in pure water is very low, even lower than that of the corresponding type I squaraines, **4414A** and **8814A**. Similar to the type I squaraines, **4414DHA** forms

Table 1. Aggregation of Squaraines in the DMSO−H_2O Mixed Solvent

squaraine	dominant species	aggregation range (DMSO%)[a]	maximum $I_a/(I_a+I_m)$[b]	isosbestic point[c]
1114A	dimer (590 nm)	0%		
	monomer (648 nm)		<10%	
4414A	dimer (594 nm)	0%	21%	yes
	↓	↓		
	monomer (650 nm)	5%		
8844A$_2$	aggregate (530 nm)	10%	53%	
		↓		no
	dimer (590 nm)	60%		
	monomer (650 nm)			
8814A	aggregate (530 nm)	40%	81%	
	↓	↓		yes
	monomer (650 nm)	65%		
4414DHA	aggregate (520 nm)	20%	83%	
	↓	↓		yes
	monomer (650 nm)	60%		
8814DHA	aggregate (520 nm)	70%	85%	
	↓	↓		yes
	monomer (650 nm)	80%		
48DHT	aggregate (520 nm)	0%	25%	
		↓		no
	dimer (588 nm)	9%		
	monomer (650 nm)			
88DHT	aggregate (520 nm)	50%	80%	
	↓	↓		yes
	monomer (650 nm)	70%		

[a] The minimum range of (DMSO% (v/v) required to observe the changes from aggregate to monomer. [b] $I_a/(I_a + I_m)$: ratio of the absorbance of aggregate to the sum of absorbance of aggregate and monomer at certain DMSO%. [c] During the conversion from aggregate to monomer at constant dye concentration.

monomeric (650 nm) complexes with α-cyclodextrin in water and dimer (585 nm) with γ-cyclodextrin. In DMSO-H_2O mixed solvent **4414DHA** and **8814DHA** form a mixture of aggregate (520 nm) and monomer (650 nm) the ratio of which is dependent on the fraction of DMSO (DMSO%). Similar to **8814A**, the aggregate−monomer conversion in both cases occurs with a clear isosbestic point indicating an equilibrium between the two species without much, if any, population of the dimer. Table 1 summarizes the range of solution composition over which the interconversion occurs; compared to the type I squaraines there is a greater percentage of aggregate in the mixed solvents as well as a persistence of aggregate to higher percentages of DMSO.

Even though type III squaraines **48DHT** and **88DHT** are designed for the study of aggregation in pure vesicles, their aggregation behavior in DMSO−water mixed solvent is also very interesting. Also shown in Table 1, the different behavior of **44DHT** and **88DHT** due to different hydrophobic chain length is clear: for the former a mixture of monomer, dimer, and aggregate is obtained even at very low percent DMSO (DMSO%) with no isosbestic point for the conversion; while for the later only monomer and aggregate are observed with a clear isosbestic point for the conversion and a much greater percentage of the aggregate as well as a higher range of DMSO%. Comparing the aggregation behavior of **48DHT** with that of **4414DHA**, it appears that introducing the quaternary ammonium salt head group in the squaraine surfactant diminishes somewhat the tendency of the squaraine to aggregate. This is probably due to the electrostatic repulsion between the positively charged head groups. In fact, addition of electrolytes such as NaCl to the solution of type III squaraines in DMSO−H_2O mixed solvent dramatically enhances the aggregate formation which can be attributed to the increase in the effective dielectric constant of the solution which reduces the electrostatic

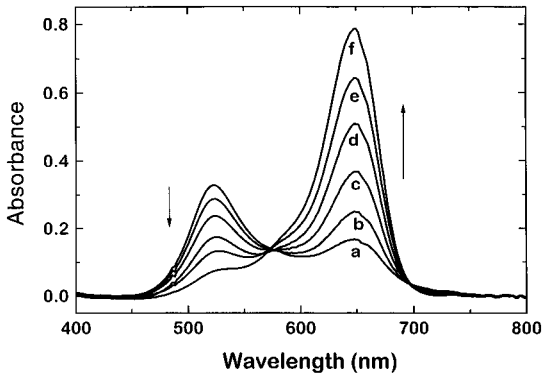

Figure 3. Absorption spectra for **4414DHA** (6.56×10^{-6} M) in DMSO−H_2O mixed solvent at different temperatures: (a)−(f) 5, 15, 25, 35, 45, 55 °C.

repulsion. In contrast, the ionic strength effect on the aggregation of type I and II squaraines is much lower than for type III.

It is important to note that for squaraines **8814A**, **4414DHA**, **8814DHA,** and **88DHT**, an equilibrium between monomer and aggregate was observed with no detectable dimer present. The monomer to aggregate conversion can be accomplished either by changing the percentage of DMSO or the solution temperature. One example is given in Figure 3 indicating the monomer−aggregate conversion of **4414DHA** at various temperatures (5−55 °C). Due to the high stability of **4414DHA**, **8814DHA**, and **88DHT** in DMSO−H_2O mixed solvent, it is possible to analyze the monomer−aggregate equilibrium carefully over a moderate temperature range for **88DHT** as has been done previously for **4414DHA** and **8814DHA** (see **Discussion**).

Microheterogeneous Media: Bilayer Vesicle Systems. Aggregation in Mixed Vesicles. The solubility of type I and II squaraines (except **1114A**) in water is significantly enhanced upon addition of the phospholipid, and a clear solution of the mixed dye and the phospholipid is obtained upon probe sonication for a proper period of time (*ca*. 15 min). Generally, the molar ratio of dye to phospholipid can reach as high as 1/1 for most type I and II squaraines with the formation of clear and stable solutions. For example, **8814A** can be incorporated as a guest into phospholipid vesicles in water. As shown in Figure 4, the absorption spectrum for relatively high ratios of squaraine to phospholipid (dimyristoylphosphatidylcholine (DMPC) or dipalmitoylphosphatidylcholine (DPPC)) shows a predominance of the blue-shifted (520 nm) aggregate similar to the spectra obtained in LB films or in DMSO−H_2O mixtures. At lower dye/DMPC ratios more contribution from the monomer spectrum is observed. Similar results for **8814DHA**/DMPC mixtures are also observed.[19] Light scattering and membrane filtration experiments have indicated that these vesicles are considerably larger than pure DMPC vesicles.[19]

Other type I and II squaraines except **8844A$_2$** have similar aggregation behavior to that of **8814DHA** and **8814A** in phospholipid vesicles. Significant amounts of **8844A$_2$** exist as monomer even at very high dye/DMPC ratio (such as 1/5). This is not surprising since the weak chromophore−chromophore interaction of **8844A$_2$** due to steric effects allows a complete dispersion of the dye as individual monomers into the phospholipid bilayers.

The coexistence of monomer, dimer, and aggregate in the mixed vesicles makes it difficult to accurately calculate the aggregation number for these squaraine aggregates formed in the bilayer systems. No pure aggregate spectra can be obtained even at very low PC/dye ratio for most of the squaraines. However, squaraine **8814DHA** can be dispersed in DMPC with relatively high dye concentration (5×10^{-5} M) at high dye/

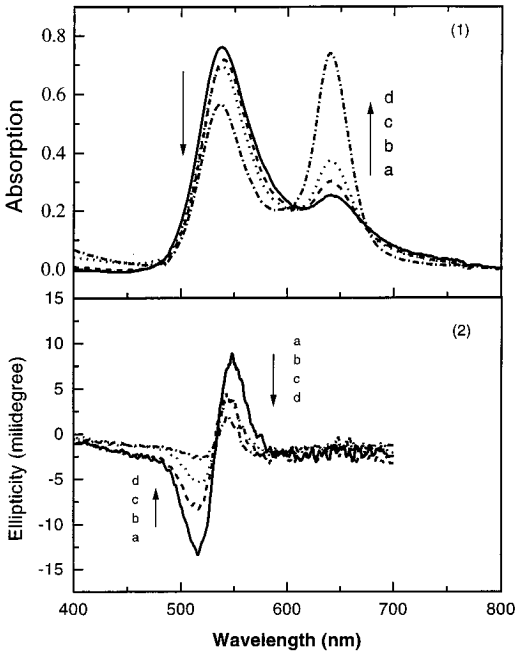

Figure 4. Absorption (1) and CD (2) spectra for **8814A** (1.0×10^{-5} M) in L-DMPC vesicles. Dye/DMPC: (a)−(d) 1/5, 1/10, 1/25, 1/50.

Chart 1 Squaraine Structures

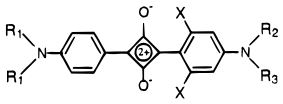

Type I

1114A: $R_1 = CH_3$, $R_2=CH_3$, $R_3=(CH_2)_3COOH$, X=H;

4414A: $R_1=C_4H_9$; $R_2=CH_3$, $R_3=(CH_2)_3COOH$, X=H;

8814A: $R_1=C_8H_{17}$, $R_2=CH_3$, $R_3=(CH_2)_3COOH$, X=H;

8844A$_2$: $R_1=C_8H_{17}$, $R_2=R_3=(CH_2)_3COOH$, X=H

Type II

4414DHA: $R_1=C_4H_9$, $R_2=CH_3$, $R_3=(CH_2)_3COOH$, X=OH

8814DHA: $R_1=C_8H_{17}$, $R_2=CH_3$, $R_3=(CH_2)_3COOH$, X=OH

Type III

48DHT: $R_1=C_4H_9$, $R_2=CH_3$, $R_3=(CH_2)_8N^+(CH_3)_3Br^-$, X=OH

88DHT: $R_1=C_8H_{17}$, $R_2=CH_3$, $R_3=(CH_2)_8N^+(CH_3)_3Br^-$, X=OH

DMPC ratio (1/2.5) to form the pure aggregate (520 nm) whose spectrum is the same in shape and absorption maximum to that obtained in DMSO−H_2O mixed solvent and in LB films. The apparent extinction coefficient for the aggregate at λ_{max} (520 nm) is *ca.* 1.1×10^5 M^{-1} cm^{-1}. The pure monomer spectrum is easily obtained from the very low concentration of dye in DMPC vesicles.

Additional information concerning the aggregate structure and aggregate incorporation into the mixed vesicles is provided by examining the circular dichroism spectra of the **8814A**/DMPC mixtures in water. When **8814A** is dispersed in L-DMPC (*R* isomer) the blue-shifted aggregate shows a strong biphasic induced circular dichroism (ICD) spectrum in the range 450−550 nm whose crossing point coincides with the λ_{max} of the major exciton band (Figure 4). As shown in Figure 4, when the ratio of DMPC to dye is increased so that appreciable amounts of dimer and monomer are present, the ICD signal still corresponds to the aggregate exciton with little or no signal corresponding to the latter two species. This is reasonable since the squaraine chromophore is achiral, and in dilute vesicles the monomer and dimer are likely too far removed from the chiral center in the phospholipid host for there to be a strong chiral perturbation of the chromophore. The observation of a strong signal from the aggregate suggests that the aggregate itself may be chiral, as has been suggested recently for other systems.[21,22] The polarity of the biphasic ICD spectrum for **8814DHA**/DPPC system was found to be dependent on the chirality of the host phospholipid (L-DPPC vs D-DPPC), with no observed ICD signal when a racemic mixture of D-DPPC and L-DPPC was used as host.[19] The ICD spectra for **8814DHA** show no change as the solutions are heated through the phase transition temperature for DPPC (43 °C).[32] Other type I and II squaraines which can also be incorporated into DMPC or DPPC vesicles show induced circular-dichroism spectra with similar biphasic features.

Aggregation in Pure Vesicles. Both squaraines **48DHT** and **88DHT** form stable large vesicles upon probe sonication (diameter 177 and 194 nm, respectively) which cannot be extruded through 100 nm filters. In contrast to the mixed vesicles in which a significant amount of monomer (indicated by the monomer fluorescence at *ca.* 655 nm in contrast to the nonfluorescent aggregate) still exists even at a high dye/phospholipid ratio, the spectrum of the pure vesicles shows a very sharp blue-shifted absorption at 520 nm which is almost the same in shape and absorption maximum as those observed in DMSO−H_2O mixed solvents and in LB films, with virtually no monomer present (supported by the lack of emission). Similar to the mixed vesicles, the aggregate can be converted to a mixture of the dimer (580 nm) and monomer (ca. 630 nm) by addition of another quaternary ammonium salt surfactant, dioctadecyldimethylammoniumbromide (DODAB), to the solution. The aggregate obtained from **48DHT** vesicles has a slightly broadened absorption compared with **88DHT**, which might be attributed to the fact that the hydrophobic chains (butyl groups) in **48DHT** are shorter and form less ordered bilayer membranes than **88DHT**.

No ICD signal was observed for pure vesicles of **48DHT** and **88DHT**. However, the quaternary ammonium salt head groups in these squaraines can electrostatically interact with negatively charged species; the formation of the complex of **48DHT** or **88DHT** with a chiral amino acid such as α-alanine is possible under slightly basic conditions (pH = 8−9). Not surprisingly, similar biphasic ICD signals which correspond to the aggregate transition were observed for the vesicles binding D- or L-α-alanine. It is obvious that the biphasic ICD behavior is a general phenomenon which relates only to the squaraine aggregate rather than the dimer or monomer species, which reinforces the concept that the squaraine aggregates are chiral.

Fluorescence Lifetime Measurements. Fluorescence decay measurements were carried out for **4414A** and **4414DHA** in a number of solvents. The results of these measurements are summarized in Table 4. All decays were biexponential, and no wavelength dependence was observed on the calculated decay parameters across the emission spectrum for all measurements except when ethanol solvent was used. Typical fluorescence decay curves (**4414A** in acetonitrile) are shown in Figure 5. Absence of wavelength dependence is illustrated by the superimposed decay curves obtained at different wavelengths in Figure 5b. Squaraine compounds studied are expected to be monomeric under the experimental conditions used for these measurements (μM concentration) as indicated by their absorption spectra. In addition, sample dilution for **4414A** in acetonitrile and chloroform did not affect the calculated decay constants. These results suggest that the biexponential nature of the fluorescence decays is not caused by intermolecular

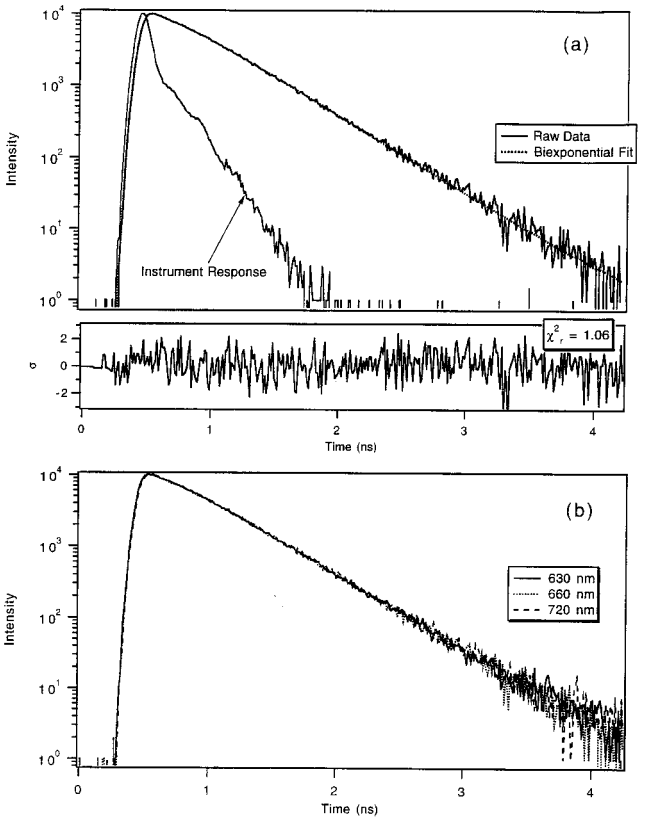

Figure 5. Fluorescence decay curves for **4414A** in acetonitrile: (a) biexponential fit and residuals for decay at 660 nm and (b) superimposed fluorescence decays at three different wavelengths.

effects such as aggregation (dimers and larger aggregates do not show any measurable fluorescence).

Transient Absorption Measurements. Excited state lifetimes for **4414A** and **4414DHA** were also measured in several solvents using picosecond transient absorption (TA) spectroscopy. The measured lifetimes were in good agreement with those from fluorescence decay measurements. However, due to the inherently higher signal/noise ratio associated with the TCSPC technique, values obtained from fluorescence decays are expected to be more reliable (Table 4). Representative differential absorption spectra for **4414A** in ethanol are shown in Figure 6 along with a biexponential fit to the recovery of the bleaching signal at 640 nm. The decay parameters for the excited state absorption in the 480 nm region and ground state bleaching band at 640 nm were identical in all cases within the experimental accuracy of the measurements. The displacement of the peak of the bleaching signal from 640 to ~650 nm in Figure 6 is due to stimulated emission. No variation in the shape or decay constants of the TA spectra were observed as a result of laser pump energy changes.

Transient absorption spectra were also obtained for squaraine aggregates formed in the **88DHT** and **8814DHA**/DMPC aqueous vesicle solutions. Complex spectral evolution was observed for these systems after the initial laser excitation. There was also strong dependence of the shape and kinetics of the spectra on laser pump intensity as can be observed in Figure 7 for the **8814DHA**/DMPC solution. The peak of the ground state bleaching band in these spectra is blue-shifted due to the presence of an overlapping absorption band in the 510−580 nm range. At all laser energies examined, the absorption band below 480 nm decayed with a deconvoluted lifetime of 30 ps. However, bleaching recovery at 520 nm appeared nonexponential and slowed with increase in laser pump energy (Figure 8). The excited state decay kinetics of fluorescent aggregated

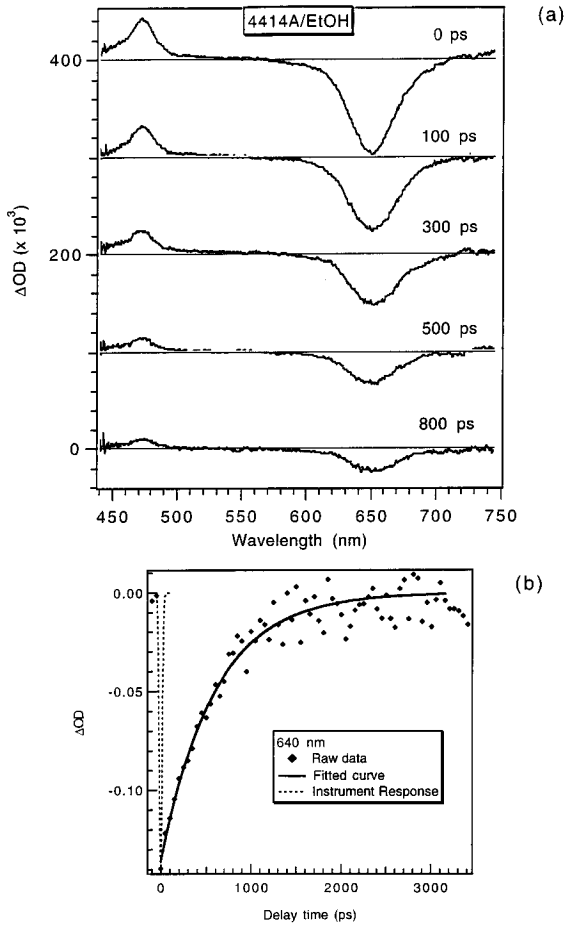

Figure 6. Transient absorption spectra after laser excitation at 532 nm (a) and bleaching recovery at 640 nm (b) for **4414A** in ethanol. The fitted curve represents a biexponential function with time constants of 120 and 600 ps.

stilbenes in microheterogeneous environments such as bilayer vesicles have also been found to be nonexponential.[33] Although it was possible to obtain reasonable biexponential fitting parameters for the decays in Figure 8, such parameters would not be based on a valid decay mechanism. Nevertheless, an initial recovery time of ~30 ps was obtained for **88DHT** and **8814DHA**/DMPC at low laser intensity (<50 μJ/plse) and deconvolution using an exponential model. Close examination of the new absorption monitored at 565 nm revealed a growth rate constant of 60 ps after deconvolution of the instrument response (150 μJ/plse, **8814DH**/DMPC). Although the magnitude of this signal increased with laser pump energy, it did not show linear or quadratic dependence on the pump energy. Similar results were observed for an aqueous vesicle solution of **88DHT**, with the exception that no excited state absorption was observed in the 510−580 nm region at low laser pump energies (<50 μJ/plse).

Discussion

Aggregation of Squaraines in water and DMSO−H_2O Mixtures. For all of the amphiphilic squaraine dyes investigated

(31) Law, K.; Bailey, F. C. *J. Org. Chem.* **1992**, *57*, 3278.
(32) Gennis, R. B. *Biomembranes: Molecular Structure and Function*; Cantor, C. R., Ed; Springer-Verlag: New York, 1989.
(33) Farahat, M. S.; Song, X.; Geiger, C.; Whitten, D. G. Manuscript in preparation.
(34) Benesi, H.; Hildebrand, J. H. *J. Am. Chem. Soc.* **1949**, *71*, 2703.
(35) Law, K. Y. *J. Phys. Chem.* **1989**, *93*, 5925.

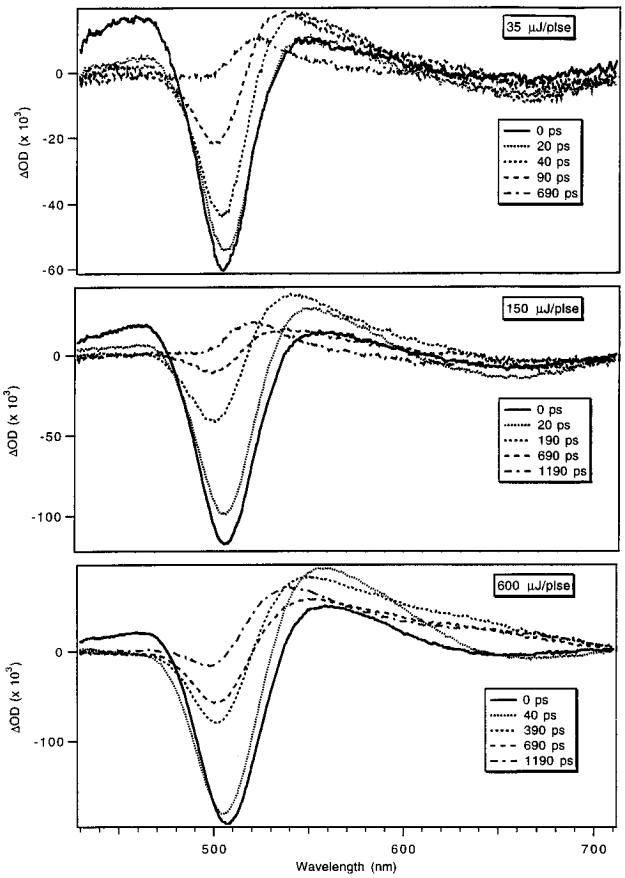

Figure 7. Time resolved spectra and laser pulse energy dependence for **8814DHA**/DMPC (1/2.5) vesicle solution.

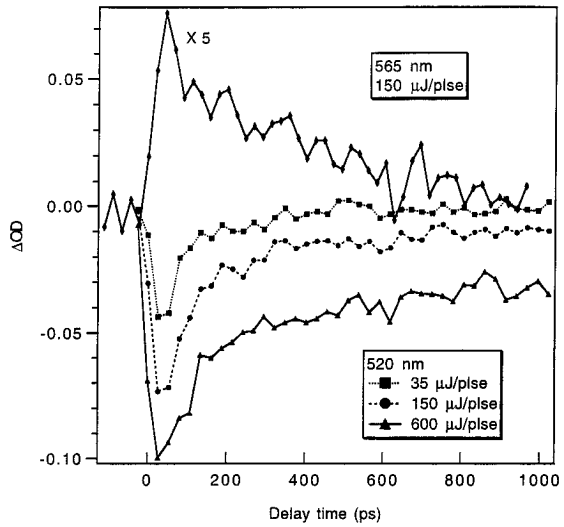

Figure 8. Decay of transient absorption and bleaching signals for **88DT** vesicle solution as a function of laser pulse energy.

in the present study it is clear that formation of similar spectrally blue-shifted aggregates is a very general process in water, in mixed aqueous organic solutions, in the presence of bilayer-forming surfactants, and in Langmuir−Blodgett films. In several cases a dimer can also be detected; the dimer generally shows an absorption blue-shifted from monomer and intermediates between the monomer and aggregate. For the different functionalized squaraines such as the "type I" squaraines, some clear trends may be noted in the tendency to form aggregates. As shown in Figure 1, the increase in alkyl chain length in the series, **1114A**, **4414A**, and **8814A**, results in an increase in the extent of aggregation at a constant dye concentration in water

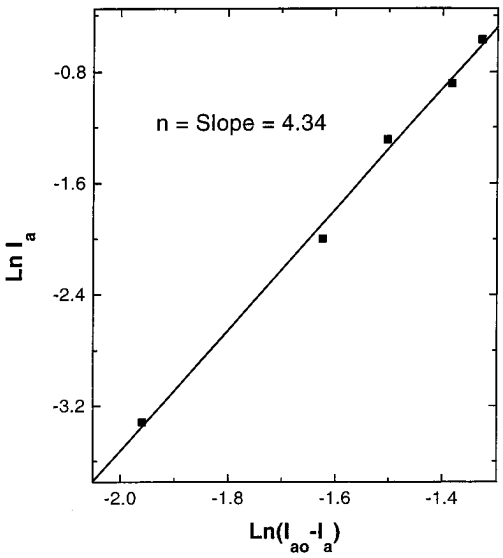

Figure 9. Benesi−Hildebrand plot of $\ln I_a$ *versus* $\ln(I_{ao} - I_a)$ of squaraine **4414DHA** in DMSO−H_2O mixed solvent with 50% (v/v) DMSO at 308 K.

("hydrophobic effects"). For the mixed DMSO−H_2O solutions a comparison of the entire series of compounds may be made by examining both the range of solution composition and the maximum extent of aggregation as indicated by the maximum value of $I_a/(I_a + I_m)$ where I_a and I_m are the absorbance values for aggregate and monomer at the respective maximum; the maximum value of this ratio is always obtained at the minimum value of the percent DMSO given in Table 1. In several cases the presence of isosbestic points during the solvent-change mediated aggregate−monomer interconversion (Figure 2(1) and 3) suggests that there is a simple equilibrium between aggregate of a discrete size and monomer. From the data presented in Table 1, it is clear that for similarly substituted squaraines of the different series, those of the type II show the highest tendency to aggregate while those of the type I and type III show lower but similar tendencies to aggregate. The higher tendency to form aggregates for the type II squaraines is readily attributed to intermolecular hydrogen bonding for the dihydroxyl derivatives.[5] In the case of the type III squaraines, some repulsion between the quaternary head groups may account for the slightly lower tendency to aggregate than that observed for the similar squaraines terminating in carboxyl groups (type II). In agreement with this postulate, we find that addition of electrolytes such as NaCl or KNO_3 in the solution enhances the aggregation of **48DHT** and **88DHT** in DMSO−H_2O mixtures.

Quantitative Analysis of Squaraine Aggregation. The equilibrium between monomer (**M**) and aggregate (**Agg**) of order *n* is represented by eq 1 and can be analyzed by the Benesi−Hildebrand treatment[34] according to eqs 2 and 3.

$$n\mathbf{M} = \mathbf{Agg} \tag{1}$$

$$K = [\mathbf{Agg}]/[\mathbf{M}]^n \tag{2}$$

$$\ln I_a = n \ln (I_{ao} - I_a) + \text{constant} \tag{3}$$

where I_a is the absorbance of **Agg** at any concentration and I_{ao} is the absorbance of pure aggregate (no monomer present). The analyses are based on two ratios: (1) $\mathbf{R_a}$, the ratio of aggregate absorbance at λ_1 (522 nm), to that at λ_2 (650 nm) which can be calculated from the pure aggregate spectrum and (2) $\mathbf{R_m}$, the ratio of monomer absorbance at the same two wavelengths,

Table 2. Equilibrium Constants and Thermodynamic Functions for 4414DHA in DMSO-H_2O Mixed Solvent (50% DMSO)

temp (K)	aggregation no. (n)	equilibrium constant K^a	$\Delta H°$ (kcal mol^{-1})	$\Delta S°$ (cal mol^{-1} k^{-1})
278	4.35	5.56×10^{20}		
288	4.01	2.93×10^{20}		
298	4.29	7.63×10^{18}	−4.20	−46.4
308	4.34	1.05×10^{18}		
318	4.21	5.64×10^{16}		

[a] Equilibrium constant in (mol^{-1} L)$^{n-1}$.

Table 3. Quantitative Results of the Aggregation of Squaraines in DMSO−H_2O Mixed Solvent

squaraine	DMSO%	n[a]	K[b]	$\Delta H°$ (kcal mol^{-1})	$\Delta H°$ (cal mol^{-1} k^{-1})
4414DHA	50	4.2 ± 0.2	7.63×10^{18}	−42.0	−46.4
8814DHA	79.5	5.2 ± 0.6	2.79×10^{21}	−40.7	−37.4
88DHT	60	3.9 ± 0.3	1.38×10^{17}	−45.5	−74.4

[a] Average aggregation number. [b] Equilibrium constant at 298 K in (mol^{-1} L)$^{n-1}$.

Table 4. Excited State Lifetimes for 4414A and 4414DHA in Different Media

medium	fluorescence decay[a] $\tau_{1\,(ps)}$	f_1[b]	$\tau_{2\,(ps)}$	f_2[b]	χ^2_r	transient absorption τ (ps)[c]
			4414A			
CH_3CN	405	0.94	45	0.06	1.06	
EtOH	650	0.95	100	0.05	1.09	600, 120
DMSO	1080	0.94	140	0.06	1.06	
$CHCl_3$	2170	0.98	168	0.02	1.03	2100, 150
H_2O	246	0.07	50	0.93	1.47	50
			4414DHA			
EtOH	268	0.85	35	0.15	1.09	220, 30
DMSO	778	0.98	74	0.02	1.01	
$CHCl_3$	268	0.92	64	0.08	1.00	260, 60

[a] Measured at or near the peak of the emission spectrum. Excitation at 590 nm. [b] Fractional contribution to total intensity at measured wavelength. [c] Exponential decay constants measured at the peak of the ground state bleaching band. Excitation at 532 nm.

which can be obtained from the pure monomer spectrum. In the case of **4414DHA**, $\mathbf{R_a}$ and $\mathbf{R_m}$ are calculated to be 5.99 and 0.023, respectively. I_a and I_{ao} at any dye concentration (C_o) can be calculated from eqs 4 and 5, while the concentrations are determined by eqs 6 and 7. I_1 and I_2 are the measured absorbance of the dye solution at λ_1 (522 nm) and λ_2 (650 nm), respectively, at any concentration.

$$I_{ao} = \epsilon_a C_o 1 \tag{4}$$

$$I_a = \mathbf{R_a}(I_1 - \mathbf{R_m} I_2)/(\mathbf{R_a} - \mathbf{R_m}) \tag{5}$$

$$[\mathbf{Agg}] = I_a/\epsilon_a C_o 1 \tag{6}$$

$$[\mathbf{M}] = C_o - n[\mathbf{Agg}] \tag{7}$$

Figure 9 shows a Benesi−Hildebrand plot for **4414DHA** in a 50% (v/v) DMSO−H_2O mixture. Table 2 summarizes values of K, n, ΔH_0°, and ΔH_0° in the same solvent mixture over the temperature range 278−318 K. Similar treatment of the aggregation of three different squaraines in DMSO-H_2O leads to the aggregation numbers collected in Table 3. The aggregation number is *ca*. 4 in each case, suggesting that a "unit aggregate" of the squaraines consists of four squaraine molecules. The aggregation number of **8814DHA** in DMPC vesicles is also estimated to be 3.5 ± 1. The relatively high stability of this "unit aggregate" compared to the dimer suggests

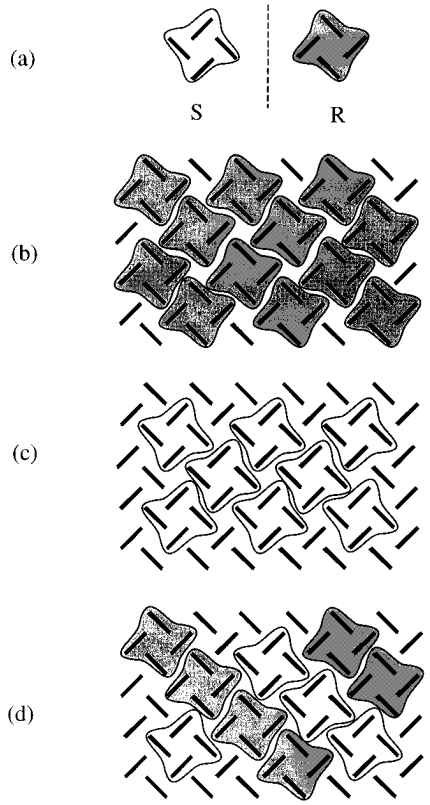

Figure 10. Schematic representation of the aggregate structures as viewed from above in the direction of molecular long axis: (a) chiral pinwheel unit aggregates with arbitrary designation of "*R*" and "*S*" enantiomers; (b), (c), and (d): glide or herringbone lattice viewed as mosaic of "all *R*", "all *S*" and a mixture of equal portion of "*R*" and "*S*", respectively.

that it must contain attractive (bonding) interactions not possible in the dimer. Taken together with the induced circular dichroism observed for the aggregation of **8814DHA** in DMPC vesicles (but not for monomer or dimer) and for the "pure" vesicles of **48DHT** and **88DHT** in the presence of chiral α-alanine enantiomers, this suggests that the unit aggregate is chiral. A structure fulfilling these requirements may be the "pinwheel" structure (Figure 10). This structure also may be extracted from Monte Carlo simulations of monolayer clusters of the squaraine acids such as **4414A** and **4414DHA**.[19] In such cases the lowest energy calculated structure which shows the best agreement between calculated and measurable properties, such as tilt angle, surface area per molecule, and exciton splittings calculated by the extended dipole treatment of Kuhn and co-workers,[13,14] is a glide plane or herringbone arrangement shown schematically in Figure 10.[19] It is quite straight forward to extract the "unit aggregate" or pinwheel structure as a primary building block for the glide or herringbone lattice. This arrangement is very similar to that concluded as the most likely structure for spectrally blue-shifted aggregates observed for other aromatic chromophores such as *trans*-stilbene and *trans*-azobenzene derivatives,[21,22] and it may well be a general supramolecular structure from which larger crystallites or aggregates may be constructed. We have discussed elsewhere[19,21] some of the factors which may contribute to the stability of the "pinwheel" structure for the unit aggregate.

It is interesting to note that while the pinwheel "unit structure" is chiral, the extended herringbone lattice is achiral. This is easily understood, as shown in Figure 10, since the same glide lattice may be constructed from a mosaic of "all *R*", "all *S*", or equal amounts of *R* and *S* unit aggregates. This leads to a simple

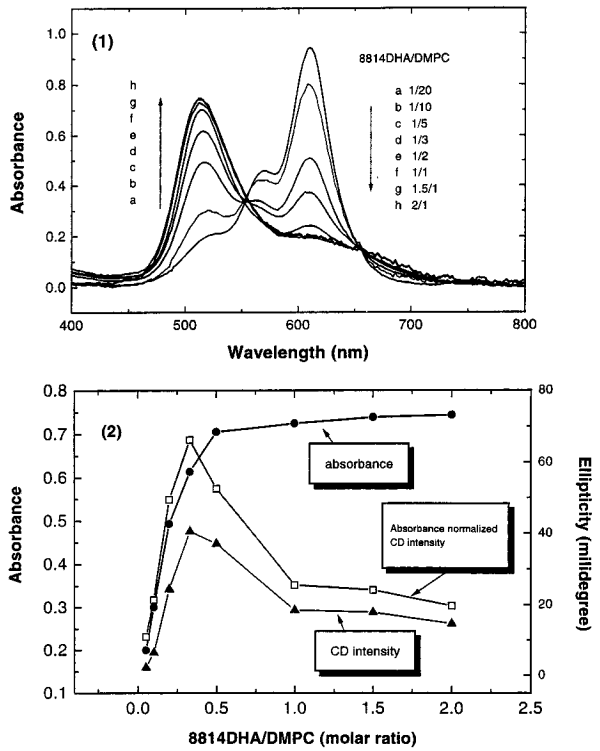

Figure 11. 8814DHA (1.0×10^{-5} M) in DMPC vesicles with various **8814DHA**/DMPC molar ratios: (1) absorption spectra and (2) plot of the absorbance at 518 nm and the ICD intensity of the mixed vesicle solution versus the **8814DHA**/DMPC molar ratio.

prediction that as chiral unit aggregates are collected to form a larger aggregate mosaic, there may be a decrease in the intensity normalized ICD signal. Interestingly we find, as shown in Figure 11, that as the conversion of unit aggregate to extended aggregate increases (in this case for **8814DHA** in DMPC as the **8814DHA**/DMPC molar ratio increases), both the overall ICD and the normalized ICD intensity decrease after an initial maximum is obtained.

Excited State Dynamics. The steady state spectroscopy and photophysics of squaraines have been studied in detail by one of the authors.[35−37] The photophysics of the squaraines in the present study are in general agreement with previous reports. In addition, due to the higher sensitivity of the time-resolved instrumentation used, an additional short-lived component for the fluorescence decays is observed. This biexponential decay suggests that there may be more than one species that contributes to the fluorescence emission.[38] Contributions from a solvent−solute complex as well as a rotational isomer to the fluoresence of monomeric squaraine dyes in solution have been reported.[36] Further characterization of the monomeric squaraines beyond that already presented was not carried out because the prime objective of this work was to investigate the properties of the aggregates.

Transient absorption spectroscopy was used to characterize the excited state behavior of the nonfluorescent aggregated species in bilayer vesicle solutions. The lifetime of the aggregate, measured by monitoring the decay of absorption at 480 nm or the initial ground state bleaching recovery at 520 nm using low laser intensities, is ∼30 ps. The intensity-dependent excited state absorption in the 510−580 nm region suggests a process involving different excited moieties.[39] Photodissiciation into monomeric squaraine, which has been reported for other dimeric squaraines in solution,[5] is not observed in the present systems.[40] In the present systems the excited state absorption in the 400−480 nm region is attributed to a transition from the one-exciton to the two-exciton level[41] in the H-aggregates of **8814DHA** and **88DHT**. The more complex spectral evolution and laser intensity dependence in the 500−580 nm region are believed to be caused by large exciton−exciton interactions that may lead to the formation of biexctons.[41,42]

Summary

The effect of molecular structure on the aggregation of amphiphilic squaraines in aqueous solution and in microheterogeneous media has been investigated. All of the amphiphilic squaraines form blue-shifted, "H" aggregates. The tendency for aggregation increases as the length of the hydrocarbon chain increases, indicative of a hydrophobic effect. While intermolecular hydrogen bonding enhances the aggregation, squaraines with quaternary ammonium head groups exhibit less tendency for aggregation probably due to electrostatic repulsion between the head groups. Experimentally, we show that the tendency for aggregation increases when an electrolyte is present in the solution. Unlike the monomeric form of squaraine, the blue-shifted aggregates are nonfluorescent and short-lived (∼30 ps). The photophysics of the aggregate is complex and remains to be elucidated. Evidence is obtained that most squaraines form aggregates without forming a dimer or a trimer first. The aggregation number can be determined by a Benesi−Hildebrand type analysis to be ∼4 for several squaraines. Taken together with the induced circular dichroism observed for the aggregate and Monte Carlo simulation results, we propose that the unit aggregate is a tetramer with a chiral "pin-wheel" structure. The extended aggregate observed in LB films and vesicles are simply a mosaic of the unit aggregates. This model is supported by observation of induced CD as a function of dye concentration in DMPC vesicles, where ICD signal is shown to decrease at high dye concentration.

Acknowledgment. We are grateful to the National Science Foundation for support of this work as part of the NSF Center for Photoinduced Charge Transfer (CHE-9120001).

JA9523911

(36) Law, K. Y. *J. Phys. Chem.* **1987**, *91*, 5184.
(37) Law, K. Y. *J. Photochem. Photobiol. A* **1994**, *84*, 123.

(38) The biexponential nature of the excited state decay may also be caused by interconversion between close-lying electronic states after the initial excitation process, in addition to the usual deactivation channels (Jones, G. II; Farahat, M. S. *Adv. Electron Transfer* **1993**, *3*, 1 and Rettig, W. *Topics Curr. Chem.* **1994**, *169*, 253). In such a case, no wavelength dependence is observed for the fluorescence decay parameters when only one of the excited states involved is emissive (Lippert, E.; Rettig, W.; Bonacic-Koutecky, V.; Miehe, J. *Adv. Chem. Phys.* **1987**, 68, 1).

(39) Multiphoton ionization may be dismissed based on the lack of quadratic dependence of the new absorption on laser intensity. Formation of dye radicals by an excited state annihilation mechanism may also be ruled out, since the observed spectra at long times after laser excitation appear only as positive bands indicating an oscillator strength greater than that of the ground state—an unlikely situation.

(40) Formation of the monomeric form would give rise to a distinctive new absorbance peak in the 640 nm region, contrary to the observed results (Figure 7).

(41) Observation of two-exciton bands in pump-probe experiments and other non-linear processes have been explored both theoretically (Spano, F. C. *Chem. Phys. Lett.* **1995**, 234, 29 and Mukamel, S. *Principles of Nonlinear Optical Spectroscopy*; Oxford University: Oxford, 1995) and experimentally (VanBurgel, M.; Wiersma, D. A.; Duppen, K. *J. Chem. Phys.* **1995**, 102, 20 and Horng, M. L.; Quitevis, E. L. *J. Phys. Chem.* **1993**, 97, 12403).

(42) In order to investigate the excitonic interactions in squaraine dyes, a model series of covalently linked dimeric squaraines has been synthesized and their steady state and time resolved properties have been investigated. The pump-probe spectra for these molecules show two-exciton absorption bands, and they can be modeled using non-linear optical response theory (see Mukamel, S. in ref 41). Farahat, M. S.; Liang, K.; Mukamel, S.; Whitten, D. G. Manuscript in preparation.